ECG Biometric Authentication Using a Dynamical Model

Abhijit Sarkar [1,2]
asarkar1@vt.edu

A. Lynn Abbott [1]
abbott@vt.edu

Zachary Doerzaph [2]
ZDoerzaph@vtti.vt.edu

[1]Bradley Department of Electrical and Computer Engineering, Virginia Tech [2]Virginia Tech Transportation Institute
Blacksburg, Virginia, USA

Abstract

This paper concerns the authentication of individuals through analysis of electrocardiogram (ECG) signals. Because the human heart differs physiologically from one person to the next, ECG signals represent a rich source of information that offers strong potential for authentication or identification. We describe a novel approach to ECG-based biometrics in which a dynamical-systems model is employed, resulting in improved registration of pulses as compared to previous techniques. Parameters at the fiducial points are detected using a sum-of-Gaussians representation, resulting in an 18-component feature vector that can be used for classification. Using a publicly available dataset of ECG signals from 47 participants, a classifier was formulated using quadratic discriminant analysis (QDA). The observed mean authentication accuracies were 90% and 97% using 100 beats and 300 beats, respectively. Although tested with standard ECG signals only, we believe that the approach can be extended to other sensor types, such as fingertip-ECG devices.

1. Introduction

Biometric authentication and identification systems have assumed increasing importance in recent years. Because of this importance, there is a continuing need to explore and develop new biometrics capabilities. Each of the different sensing modalities, including traditional iris-based and fingerprint-based approaches, exhibits particular strengths and weaknesses [10, 17]. The interest in this paper is authentication based on electrocardiogram (ECG) signals (Figure 1). ECG-based biometrics represents an emerging modality that has strong potential to complement or supplement existing biometrics approaches.

An ECG represents electrical activity that causes contraction of cardiac muscle fibers [12]. For example, a single pulse is shown in Fig. 1. Because the geometry and physiology of the heart differ from one individual to another [5], and because of variations in conductivity within the body, it may be possible to distinguish different individuals based on observed electrical activity.

Authentication systems that depend on signals from an individual's heart are attractive because of universality (the signals are present in all living individuals), and because the signals are difficult to falsify (as they derive from the autonomic nervous system, ANS). Traditionally, an ECG is obtained using electrodes that are placed on the surface of the body, measuring the potential difference between 2 electrodes. All the signals tested in this paper are obtained using these common techniques. However, it is possible that new sensing approaches such as fingertip-based ECG devices [3, 16] may also benefit from this work.

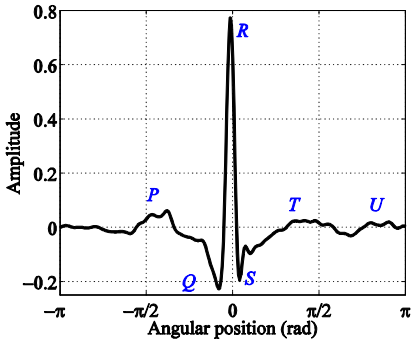

Figure 1. Example ECG pulse showing six fiducial points, designated *P* through *U*. A sum-of-Gaussians model is used in this paper to represent ECG pulses. The horizontal axis represents angular location within a dynamical model.

2. Background

Research in ECG-based biometrics can broadly be divided into two major categories: those depending on the detection of fiducial points, and those based more broadly on appearance of the signal. In fiducial based methods, the emphasis is on detection of particular distinctive parts of the ECG signal. By convention, the labels $\{P, Q, R, S, T, U\}$ are assigned as shown in Figure 1. Biel et al. [1], Israel et al. [9], Kyoso and Uchiyama [11], Irvine and Israel [7], and Singh and Singh [19] have used all or a subset of these six fiducial points for ECG biometrics. These algorithms rely on careful localizations of fiducial points. Hence the performance of these methods largely depends on the accuracy of the fiducial point detection.

An appearance based model, on the other hand, does not rely on exact localization of characteristic points. In general, these algorithms align several ECG beats by their *R* peaks and apply different time domain and frequency domain operations to extract feature vectors. Wubbeler et al. [21] have used a simple distance based classifier on the temporal derivative of the ECG signal. Temporal

autocorrelation (AC) [16, 20], discrete cosine transform (DCT)[20], wavelets [2], eigendecomposition [8], and short term Fourier transform [14] are some of the notable strategies that have been applied for feature selection. Odinaka et al. [15] have given a comparative review for various feature selection strategies and classification methods used in ECG biometrics.

In both cases, the biometric attributes are dictated by the morphology of the ECG signal. To the best of our knowledge, no prior work utilizes an analytical model to study this morphology in the context of biometric identification. We have used a dynamical system to model the ECG signal as a function of time and instantaneous heart rate. The model parameters can be used with a discriminant classifier to identify and authenticate human subjects. We have introduced a new alignment strategy for the ECG signals by using relative angular position from the *R* peak. This is in contrast to conventional time-based alignment.

3. Dynamical model: ECG morphology

Figure 2 shows one single sinus cycle of the ECG signal. One such cycle or beat can be broadly divided into two phases, known as depolarization and repolarization of the heart muscle fibers. The *P* wave is caused by the atrial depolarization, whereas the *QRS* waves are caused by ventricular depolarization. The *T* and *U-wave*, on the other hand, are the result of ventricular repolarization. The balance between the sympathetic and parasympathetic nervous system determines the variability of the heart rate. Therefore if we assume the heart as an electromechanical system in a black box, the nervous system governs the actuation signals, determining the heart rate. In this paper we replace the black box by the dynamical model proposed by McSharry et al. [12]. We consider the parameters of the dynamical model to be the characteristic features of a person. If the system can reliably estimate these parameters and capture their changing behavior, biometric authentication is possible.

Following the nonlinear dynamical model proposed by [12], we have modeled the ECG signal in three coupled differential equations:

$$\begin{aligned}\dot{x} &= \alpha x - \omega y \\ \dot{y} &= \alpha y + \omega x \\ \dot{z} &= \sum_{i\in\{P,Q,R,S,T,U\}} -a_i \Delta\theta_i \exp\left(-\frac{\Delta\theta_i^2}{2b_i^2}\right) - (z - z_0)\end{aligned} \quad (1)$$

where (x, y, z) represent a parametric reference frame, $\alpha = 1 - \sqrt{x^2 + y^2}$, $\theta = \tan^{-1}(y/x)$ the angular position $(-\pi \le \theta \le \pi)$, and $\Delta\theta_i = (\theta - \theta_i) \bmod 2\pi$. The dynamics of x and y traces a limit cycle of angular velocity ω. The third dimension when plotted against time gives the quasi-periodic ECG signal which is usually measured and commonly known. Depending on the relative angular position in the limit cycle, the dynamics of z decides its distance from the attractor in the *x*-*y* plane. Each of the *PQRSTU* complexes shown in Figure 2 are represented as Gaussian functions with amplitude a_i, mean θ_i, and variance b_i ([12] reported *PQRST* complex only). The value z_0 is the contribution from the baseline low frequency signal governed by the respiratory sinus arrhythmia (RSA). A typical ECG signal and its phase-wrapped trace in the 3D model space are shown in Figure 2. It is often argued that the change in heart rate has influences on the amplitude of the *R*-peak. In the current scenario we have normalized the amplitude of a single ECG cycle for simplicity and generalization.

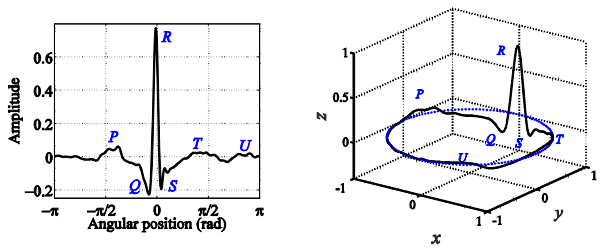

Figure 2. A typical ECG signal and its phase-wrapped version in (x, y, z) plane. The (x, y) axes denote the *cosine* and *sine* function value for each angular position in the limit cycle. Values on the *z* axis are the ECG signal.

4. Preprocessing

4.1. Noise filtering

The ECG signal is often contaminated with high frequency and low frequency noise. The low frequency noise is mainly incorporated into the baseline electrical potential (< 1 Hz). The high frequency component of ECG signal is affected by the power line frequency (60 Hz) and measurement noise from the signal lead (> 40 Hz). Using a standard filtering strategy from [20], we have employed a notch filter of 60 Hz to eliminate the power-line frequency, and a 4th order band-pass filter with passband of 1 Hz to 40 Hz.

4.2. ECG alignment by angular position

After the raw ECG signal has been filtered for noise, we have used a peak detection algorithm to identify the *R*-peaks. According to the dynamical model, each ECG beat traces the unit limit cycle once. Therefore, starting from one *R*-peak, the signal traverses 2π radians in the *x*-*y* plane to reach the next *R*-peak. In all previous research the alignment has been performed in the time domain by aligning only the *R*-peak from each single beat. Alignment for the rest of the signal is assumed to be automatic. In contrast, we have aligned each ECG signal by its relative angular position (θ) from the *R* peak. The angular positions 0 to 2π (alternatively, $-\pi$ to π) are quantized into 360 divisions. This aligns all the data points of an ECG signal to a fixed framework, and reduces the average variance in the

signal by 23%. Finally, we normalize the peak to peak amplitude for each beat to unit height (*Q*-*R* in Figure 2).

5. Parameter estimation of ECG complex

The dynamic equations in (1) can be transformed into polar coordinates [18]:

$$\dot{r} = r(1-r)$$
$$\dot{\theta} = \omega$$
$$\dot{z} = \sum_{i\in\{P,Q,R,S,T,U\}} -a_i \Delta\theta_i \exp\left(-\frac{\Delta\theta_i^2}{2b_i^2}\right) - (z - z_0) \quad (2)$$

This transformation makes the first two equations obvious and the dynamics of r redundant to current analysis. Also, for the problem of interest, we align an ECG signal by individual beats. Hence, we can ignore the baseline term $(z - z_0)$. This leaves the dynamics of z as only a simple derivative of a sum of Gaussians, and it is possible to get an analytical solution of z from (1):

$$z = \sum_{i\in\{P,Q,R,S,T,U\}} \alpha_i \exp\left(-\frac{(\theta-\theta_i)^2}{2b_i^2}\right) \quad (3)$$

where $\alpha_i = f(a_i, b_i, \omega)$ is the amplitude of the Gaussian function.

For a given ECG cycle with known angular position, $\theta_k = \omega t_k$, z can be assumed as a direct function of θ and it is possible to estimate the model parameters, $\{\alpha_i, b_i, \theta_i\}$, by formulating an optimization problem that minimizes the squared error between each observation $s(\theta_q)$ and model output $z(\theta_q)$:

$$\{\boldsymbol{\alpha}, \boldsymbol{b}, \boldsymbol{\theta}\} = \underset{\alpha_i, b_i, \theta_i}{\operatorname{argmin}} \sum_{\theta_q} \left\| s(\theta_q) - z(\theta_q) \right\|_2^2 \quad (4)$$

We have used the Levenberg-Marquardt algorithm for a non-linear least squares optimization, as implemented in Matlab. The initial estimates of the parameters for the normalized ECG signal are shown in Table 1.

Before computing the parameters we prepare an ECG template. Each template comprises n consecutive heart beats. The ECG signal for n beats are aligned by their relative angular position from the *R* peak. Figure 3 shows one such template for $n = 30$. Clearly, the template has a variation for each of the quantized angular position. To include the variation in the signal, we perform the parameter estimation in two steps. First we calculate the mean signal as shown in Figure 3, and estimate parameters for the mean signal through the minimization problem in (4). Figure 4 shows the mean signal of a template and its

Table 1. Initialization for parameter estimation.

Index	*P*	*Q*	*R*	*S*	*T*	*U*
α_i	0.12	-0.25	1.2	-0.25	0.12	0.12
b_i	$\pi/16$	$\pi/16$	$\pi/16$	$\pi/16$	$\pi/16$	$\pi/16$
θ_i	$-\pi/2$	$-\pi/16$	0	$\pi/16$	$\pi/3$	$2\pi/3$

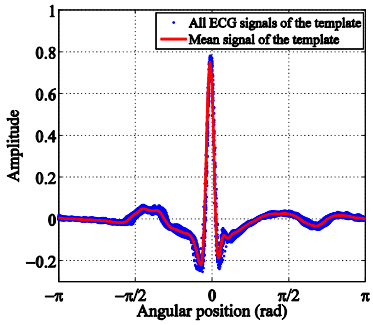

Figure 3. All the ECG signals for the thirty beats of a template and their statistical mean for each angular position.

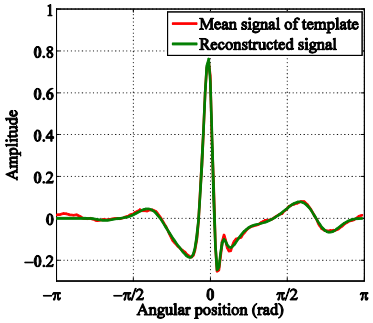

Figure 4. An example of the mean signal from a template and its reconstructed version after parameter estimation.

reconstructed version after the parameter estimation.

In the second part, we use this initial estimation and formulate another minimization problem to include the variation between each beat in a given template by (5):

$$\{\boldsymbol{\alpha}', \boldsymbol{b}', \boldsymbol{\theta}'\} = \underset{\alpha_i, b_i, \theta_i}{\operatorname{argmin}} \sum_{p=1}^{n} \sum_{\theta_q} \left\| s_p(\theta_q) - z(\theta_q) \right\|_2^2 \quad (5)$$

$s_p(\theta_q)$ denotes the signal value of p^{th} signal in the template at angular position θ_q. The second step helps the system to adapt to the variation in heart rate. This can also be thought of an approach to minimize the modeling noise. It is to be noted that a large value of n will lead towards a conservative algorithm, and requiring a large number of samples to authenticate.

6. Quadratic discriminant classification

We have tested with three classifiers: linear discriminant classifier, k-nearest neighbor and quadratic discriminant classifier (QDC). After performing 10-fold cross-validation for all the three classifiers, we observed the best result for QDC. Formally, for any given set of observation pairs (x_i, y_i), where $x_i \in \mathbb{R}^n$ is the feature vector for i^{th} example and $y_i \in \{1, \ldots, K\}$ is the i^{th} class label, we assume that the feature vectors have a multivariate Gaussian distribution. The QDC trains to find the distinct mean and variance for each of the classes in the n dimension feature space. For us, $n = 18$, $K = 47$.

For a uniform prior distribution of the classes, we test our observation to minimize the misclassification cost:

$$\hat{y} = \underset{y=1,\ldots,K}{\operatorname{argmin}} \sum_{k=1}^{K} P(k|x)C(y|k) \quad (6)$$

where $\hat{y}$ is the predicted class, the posterior probability $P(k|x)$ is defined by the prior probability (uniform in this case) and the likelihood given by multivariate Gaussian density function:

$$P(x|k) = \frac{1}{(2\pi|\Sigma_k|)^{\frac{1}{2}}} \exp\left(-\frac{1}{2}(x-\mu_k)^T\Sigma_k^{-1}(x-\mu_k)\right) \quad (7)$$

and the cost function $C(y|k)$ by an indicator function,

$$C(y|k) = \begin{cases} 1 & \text{if } y_k = k \\ 0 & \text{if } y_k \neq k \end{cases} \quad (8)$$

The terms μ_k and Σ_k are the learnt multivariate mean vector and multivariate co-variance matrix for class k.

7. Experiments and results

7.1. Dataset

We have used the MIT-BIH Arrhythmia database [13] to test the authentication process. This dataset is freely available from physionet.org [4]. It comprises records from 47 participants (25 men and 22 women with age between 23 and 89 years), each with an average of 30 minutes using a single lead ECG signal, digitized at 360 Hz. All the records are filtered using the methods described in section 4.1. We have divided each signal into templates of n beats and we estimated the parameters that best matches the template. The value of n is selected from:

$$n \in \{1,5,10,20,30\} \quad (9)$$

We test the algorithm for different numbers of training and testing beats to record its accuracy for identification and authentication. First, for any given subject j, we divide the full ECG signal into m_j templates, $\mathcal{T}_n^j(k)$, each comprising n beats and $k = 1..m_j$. After preprocessing and alignment, we estimate the 18 parameters from each of the template using (3), (4), and (5). So, for a given subject we have m_j observations and the feature vector for the j^{th} subject is $\mathcal{F}_n^j \in \mathbb{R}^{(m_j \times 18)}$. Next, we take equal number of samples, N_{train}, from each subject to train the classifier and equal number of test samples, N_{test}, all randomly chosen from each subject. The training and testing sets are disjoint with no overlap between them.

$$N_{train} + N_{test} < \min_j(m_j) \quad (10)$$

For each $\{N_{train}, N_{test}\}$ we run the test 45 times and take an average over all the results. The number 45 was chosen as an arbitrary number close to the number of subjects, 47.

7.2. Authentication results

The authentication procedure takes N_{train} templates from

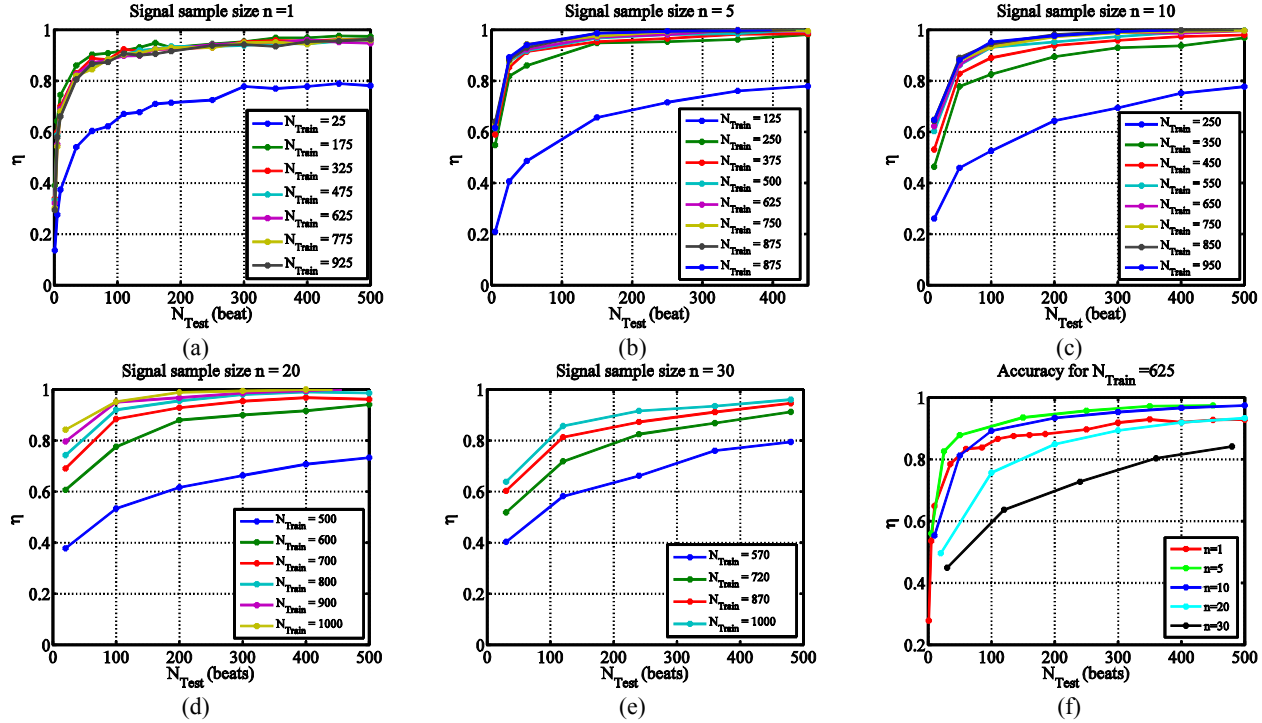

Figure 5. Authentication results: with different numbers of heart beats in training and testing. Feature vectors are extracted from a batch of (a) n=1, (b) n=5, (c) n=10, (d) n=20, (e) n=30, heart beats respectively. (f) shows a comparison of all the five templates when training is performed on 625 heart beats per subject. For these tests, a template comprising a 5-beat ECG signal provides the best authentication accuracy.

each subject and classifies each template individually. The final class is chosen by voting from each of the templates. The probe templates are assigned to the class that observes the largest number of votes. We check if individual classes are correctly identified for the given template set from each class. The authentication accuracy is given by:

$$\eta_{Auth} = \frac{Correctly\ identifed\ subjects}{Total\ number\ of\ subjects} \quad (11)$$

Figure 5 shows results for mean authentication accuracy values using different template sizes. Parts (a) – (e) show accuracy values for different numbers of training samples (varying from 25 to 1000) and testing samples (varying from 1 to 500 beats). Although we have used templates of different sizes (n), we have represented all results in number of heart beats ($number\ of\ templates \times template\ size$) for illustration. It has been noticed that with the increase of number of training samples, the accuracy also increases, but eventually saturates. We observed that templates of size $n = 5$ outperforms all other templates for most of the training and testing combinations. Figure 5(f) shows a performance comparison for a fixed training size of 625 beats. With N_{Test} more than 300, we observed accuracy of $(97 \pm 2.3)\%$, where 97% is the mean accuracy and 2.3% is the maximum deviation. For $N_{Test} = 50$, we observed an accuracy of $(90 \pm 2.1)\%$.

7.3. Identification results

The initial part of the identification test is performed in the same way as the authentication process. We vary the number of training samples and testing samples for each subject and run the classifier. From the posterior probability matrix of the classification, we compute the confusion matrix for each rank of recognition. This shows the number of testing sample correctly classified with an accuracy measurement:

$$\eta_{Iden} = \frac{Correctly\ identifed\ testing\ samples}{Total\ number\ of\ test\ samples} \quad (12)$$

It was observed that for a fixed number of training samples, identification accuracy does not change much with the change in the number of testing samples. This invariance demonstrates the stability of the algorithm. Figure 6 shows one such case for 200 training templates of size $n = 5$ (1000 beats) taken from each subject. The identification accuracy does not change appreciably up to rank 15 when we change our test template population from 5 beats to 500 beats. On the other hand, when we vary the size of the training set but fix the number of N_{Test}, we observe some increase in rank accuracy. When we used a fixed $N_{test} = 5$ beats and vary the training set size from 250 to 1000 beats using a 5 beat template, we can achieve rank 1 accuracy of 65% and rank 15 accuracy of 95%.

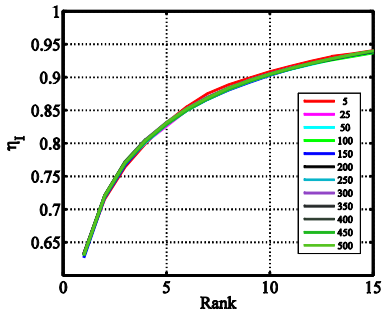

Figure 6. Identification accuracy with fixed training sample $N_{Train} = 1000$ beats and variation in N_{Test} from 5 to 500 templates each with 5 beats. η_I does not change with variation in test sample size.

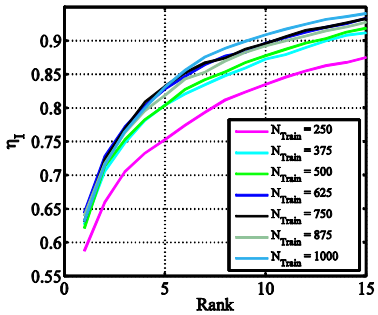

Figure 7. Identification accuracy for a fixed test size of 5 beats and varying training size from 250 to 1000 beats.

Table 2. Comparison with other studies.

Study	*Sample size*	*F/NF*	η_{Auth}
Wang et al. [20]	13	F	100%
Wang et al. [20]	13	NF	98%
Odinaka et al. [14]	269	NF	99%
Israel et al. [9]	29	F	97-98%
Irvine et al. [6]	104	F	91%
Ours	47	F	$97\% \pm 2.3\%$

Table 3. A comparison on feature space dimension.

Methods	*Initial feature space (Final)*
Irvine et al.[7]	10 - 250
Odinaka et al.[14]	2048
Wang et al. [20]	300
Raj et al. [16]	300 (10)
Ours	18

7.4. Discussion

The authentication accuracy has been often referred as subject recognition rate or identification performance, whereas the identification accuracy is referred as window matching accuracy (same as our template) or heartbeat recognition rate in different literatures. Table 2 shows a comparison with the state of the art algorithm for authentication accuracy for within session ECG records and our algorithm produces comparable results. We have used an 18 dimensional feature space for the QDC. This is

comparatively lower than most of the recent works. Table 3 compares the dimensionality of the feature space used in literature.

8. Conclusions

This paper has described a new approach for recognizing individuals using ECG signals. Although the potential for ECG-based biometric identification has been discussed for roughly 15 years, our algorithm is the first (to our knowledge) to employ an analytical approach to the problem. We have described a novel biometric algorithm in which a dynamical-system have been used to model ECG signal. We have introduced an angular position based ECG alignment strategy in contrast to the time based alignments used previously. Our method can be considered to be closer to the fiducial based methods in which the feature parameters of the six fiducial points are learned using a sum-of-Gaussians representation, resulting in an 18-component feature vector that is used for classification.

Using a classifier based on quadratic discriminant analysis (QDA), and using a heartbeat template, our system achieved an accuracy level for human subject authentication of average 97%. This method is comparable with state of the art as shown in Table 2. The analytical model [12, 18] has proved effective in noise elimination using an extended Kalman filter or unscented Kalman filter. Future work will explore the possibility of better noise elimination, as well as performance of our technique when using ECG signals from different sessions, and consideration of heart rate variability.

References

[1] L. Biel, O. Pettersson, L. Philipson, and P. Wide, "ECG analysis: a new approach in human identification," *Instrumentation and Measurement, IEEE Transactions on,* vol. 50, pp. 808-812, 2001.

[2] A. D. Chan, M. M. Hamdy, A. Badre, and V. Badee, "Wavelet distance measure for person identification using electrocardiograms," *Instrumentation and Measurement, IEEE Transactions on,* vol. 57, pp. 248-253, 2008.

[3] H. P. Da Silva, A. Fred, A. Lourenco, and A. K. Jain, "Finger ECG signal for user authentication: Usability and performance," in *Biometrics: Theory, Applications and Systems (BTAS), IEEE Sixth International Conference on*, pp. 1-8, 2013.

[4] A. L. Goldberger, L. A. Amaral, L. Glass, J. M. Hausdorff, P. C. Ivanov, R. G. Mark, J. E. Mietus, G. B. Moody, C. K. Peng, H. E. Stanley, "Physiobank, physiotoolkit, and physionet components of a new research resource for complex physiologic signals," *Circulation,* vol. 101, pp. e215-e220, 2000.

[5] R. Hoekema, G. J. Uijen, and A. van Oosterom, "Geometrical aspects of the interindividual variability of multilead ECG recordings," *Biomedical Engineering, IEEE Transactions on,* vol. 48, pp. 551-559, 2001.

[6] J. Irvine, S. Israel, M. Wiederhold, and B. Wiederhold, "A new biometric: human identification from circulatory function," in *Joint Statistical Meetings of the American Statistical Association, San Francisco*, 2003.

[7] J. M. Irvine and S. A. Israel, "A sequential procedure for individual identity verification using ECG," *EURASIP Journal on Advances in Signal Processing,* vol. 2009, no. 3, 2009.

[8] J. M. Irvine, S. A. Israel, W. T. Scruggs, and W. J. Worek, "eigenPulse: Robust human identification from cardiovascular function," *Pattern Recognition,* vol. 41, pp. 3427-3435, 2008.

[9] S. A. Israel, J. M. Irvine, A. Cheng, M. D. Wiederhold, and B. K. Wiederhold, "ECG to identify individuals," *Pattern recognition,* vol. 38, pp. 133-142, 2005.

[10] A. K. Jain, A. Ross, and S. Prabhakar, "An introduction to biometric recognition," *Circuits and Systems for Video Technology, IEEE Transactions on,* vol. 14, pp. 4-20, 2004.

[11] M. Kyoso and A. Uchiyama, "Development of an ECG identification system," in *Engineering in Medicine and Biology Society. Proceedings of the 23rd Annual International Conference, IEEE*, pp. 3721-3723, 2001.

[12] P. E. McSharry, G. D. Clifford, L. Tarassenko, and L. A. Smith, "A dynamical model for generating synthetic electrocardiogram signals," *Biomedical Engineering, IEEE Transactions on,* vol. 50, pp. 289-294, 2003.

[13] G. B. Moody and R. G. Mark, "The impact of the MIT-BIH arrhythmia database," *Engineering in Medicine and Biology Magazine, IEEE,* vol. 20, pp. 45-50, 2001.

[14] I. Odinaka, P.-H. Lai, A. D. Kaplan, J. A. O'Sullivan, E. J. Sirevaag, S. D. Kristjansson, A. K. Sheffield, and J. W. Rohrbaugh, "ECG biometrics: A robust short-time frequency analysis," in *Information Forensics and Security (WIFS), IEEE International Workshop on*, pp. 1-6, 2010.

[15] I. Odinaka, P.-H. Lai, A. D. Kaplan, J. A. O'Sullivan, E. J. Sirevaag, and J. W. Rohrbaugh, "ECG biometric recognition: A comparative analysis," *Information Forensics and Security, IEEE Transactions on,* vol. 7, pp. 1812-1824, 2012.

[16] P. S. Raj, S. Sonowal, and D. Hatzinakos, "Non-negative sparse coding based scalable access control using fingertip ECG," in *Biometrics (IJCB), IEEE International Joint Conference on*, pp. 1-6, 2014.

[17] A. Ross and A. Jain, "Multimodal biometrics: An overview," in *Proc. XII European Signal Processing Conf.*, 2004.

[18] R. Sameni, M. B. Shamsollahi, C. Jutten, and G. D. Clifford, "A nonlinear Bayesian filtering framework for ECG denoising," *Biomedical Engineering, IEEE Transactions on,* vol. 54, pp. 2172-2185, 2007.

[19] Y. N. Singh and S. K. Singh, "Evaluation of electrocardiogram for biometric authentication," *Journal of Information Security,* vol. 3, pp. 39–48, 2011.

[20] Y. Wang, F. Agrafioti, D. Hatzinakos, and K. N. Plataniotis, "Analysis of human electrocardiogram for biometric recognition," *EURASIP journal on Advances in Signal Processing,* vol. 2008, p. 19, 2008.

[21] G. Wübbeler, M. Stavridis, D. Kreiseler, R.-D. Bousseljot, and C. Elster, "Verification of humans using the electrocardiogram," *Pattern Recognition Letters,* vol. 28, pp. 1172-1175, 2007.